# EFFECT OF TOOL GEOMETRY AND PROCESS PARAMETERS ON MATERIAL FLOW IN FSW OF AN AA 2024-T351 ALLOY

**R. Zettler[1], S. Lomolino[1], J. F. dos Santos[1], T. Donath[1], F. Beckmann[1], T. Lippman[1], D. Lohwasser[2]**
**[1]GKSS-Forschungszentrum Geesthacht,**
**[2]Airbus Deutschland GmbH**
**(Germany)**

## ABSTRACT

In this study the temperature distribution and the flow pattern of an embedded marker material were investigated when friction stir butt welding 4 mm thick 2024-T351aluminium alloy plate using several welding tool combinations. Friction stir welded plates not embedded with the marker material were tested for micro-hardness and static tensile strength. Results indicated that the ultimate tensile strength of the friction stir welded material could be increased to values approaching that of the base material. The improvement in mechanical strength was found to depend largely on tool geometry in conjunction with weld travel speed. Tool geometry not only influenced the temperatures and micro-hardness experienced for both sides of the weld but also the marker material flow during joining. A micro-computer tomographic investigation of the marker flow indicated that the geometry of the welding tool pin had a significant influence on the material transport and distribution between each side of the interfacing workpieces.

***IIW-Thesaurus keywords:*** *Friction Stir Welding; Aluminium alloys; Light metals; Butt welds; Temperature; Mechanical tests; Tensile tests; Ultimate tensile strength; Mechanical properties; Strength; Elongation; Comparisons; Practical investigations.*

## 1 INTRODUCTION

Friction Stir Welding (FSW) is a solid state joining process i.e. no bulk melting of the base material occurs during joining. The process was developed and patented by The Welding Institute (TWI) of Cambridge, England [1]. The process essentially relies on frictional heating and plastic deformation of the workpieces brought about by the interaction of a non consumable and rotating tool with that of the interfacing surfaces to be joined. The joining tool consisting of a shoulder and pin is essentially plunged into and then traversed along the join line between typically two abutting workpieces. Intimate contact between the tool and workpiece surfaces causes material in the immediate vicinity of the tool to soften, flow and mix. A schematic of the process can be found in Figure 1.

As a result of FSW thermally softened material flows around the tool in the direction of tool rotation [2]. Nomenclature dictates that the side of the workpieces having the same rotation and travel direction is termed the advancing or shear side (As) while the side where travel direction and rotation are opposite is termed the retreating or flow side (Rs). The induced material flow produces what some researchers have described as an onion like structure occurring in the weld nugget [3]. Unlike fusion welding there is no evidence of an as cast microstructure across the weld region. Rather the plastic deformation that takes place within the weld nugget results in recrystallisation of the parent material grains. The outcome is a much finer and equiaxed microstructure than previously existed for the base material Surrounding the weld nugget can be found a thermo-

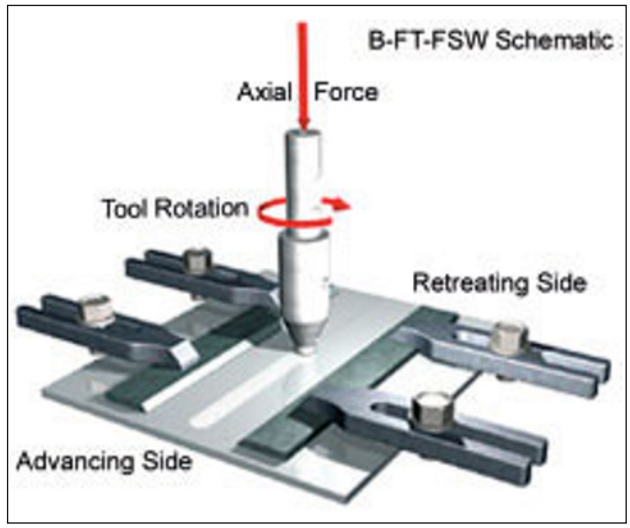


**Figure 1 – Schematic of the FSW process**

Doc. IIW-1678-05 (ex-doc. III-1301-04/IX-2121-04) recommended for publication by Commission III “Resistance welding, solid state welding and allied joining processes” and Commission IX “Behaviour of metals subjected to welding”.

mechanically affected zone (TMAZ) and then a heat-affected zone (HAZ) before one comes back into contact with the parent material.

The process of FSW has demonstrated many advantages; these include the production of high quality joints with little preparation of the joint surfaces or post-weld dressing, relatively fast production i.e. joining speeds, high fatigue strengths and the ability to join dissimilar alloys. The many advantages can be attributed to the much reduced level of heat input. Heat input has a significant influence on workpiece distortion. Moreover, the absence of melting eliminates porosity and hot cracking, problems that have been shown to occur when fusion welding aluminium and its alloys [4].

To date very considerable investment has been made in the pursuit to better understand the mechanisms of joint formation which lie at the heart of the FSW process. This is no more evident than when one considers the numerous papers published in recent years concerning heat, material flow and microstructure evolution for friction stir welds.

Geometric and microstructural differences within the join zone for both sides of a friction stir welded joint arise because the deformation process is generally not symmetric about the weld join line. Inherent differences exist between the translation and rotational velocities produced when the welding tool pin is traversed along and through the weld joint. During FSW the differences in processing velocities between each side of the weld joint increase with increased weld travel speed. As a consequence processing temperatures for each side of the weld joint are also affected. Heat and deformation not only give rise to thermal softening of the workpiece material in close proximity to the welding tool but are also responsible for the material undergoing a torturous deformation path which is not yet fully understood. This work has been undertaken in response to better understand what influence, if any, tool pin geometry has, in inducing material flow and thereby influencing the mechanical properties of a friction stir butt welded 2024-T351 aluminium alloy.

## 2 WELDING PROCESS AND WELDING TOOLS

Experiments were performed on 4 mm thick 2024-T351 aluminium. All welds were produced as butt welds where each specimen measured 110 mm in width × 400 mm in length. Welds were produced at the GKSS-Forschungszentrum using a Tricept TR 805 robot, Figure 2.

The Tricept TR 805 robot is essentially a 5 axis CNC controlled robot designed for high speed milling applications where a high degree of stiffness and flexibility is required. All movements of the robot are controlled by a Siemens Sinumeric 840D controller. Load control i.e. axial or downforce actuation and rotation speed are controlled by a separate computer system developed at the GKSS-Forschungszentrum.

FSW experiments were conducted for three welding tool pins and two shoulder profiles. All tool pins, hereafter


**Figure 2 – Tricept TR 805 Robot**

classified as pins A, B and C were based on one single profile, that being pin A, a conical non threaded pin. Pin B and pin C varied from pin A only in that pin B possessed a continuous thread over the tapered length of the pin, while pin C was an identical copy of pin B but had three flats milled at a spacing of 120° over this same length. All pins measured 5 mm in diameter for the pin shank and were produced from the same base material.

Welding tool shoulders, hereafter classified as shoulder 1 and shoulder 2 were made of the same material used to produce the tool pins. Shoulder 1 possessed a concave profile and was investigated tilted away from the direction of welding at an angle of 2.5°. Shoulder 2 possessed a spiral profile and was investigated using a tool tilt angle of 0°. The tool shoulder diameter for both shoulders measured 15 mm. During the welding process workpieces were clamped against the work table of the robot onto a steel backing bar. Tool rotation speed was held constant at 800 rpm and weld travel speed was set at 100, 200 or 400 mm/min. Downforce or axial load was maintained at 12 kN or 9 kN for the entire weld length dependant on tool configuration, see Table 1.

**Table 1 – Summary of tool configuration and weld parameter investigation**

| Shoulder / Pin type | Rot. speed (rpm) | Travel speed (mm/min) | Down-force (kN) | Tool tilt angle (degrees) |
|---|---|---|---|---|
| 1A | 800 | 100 | 12 | 2.5 |
| 1A | 800 | 200 | 12 | 2.5 |
| 1A | 800 | 400 | 12 | 2.5 |
| 1B | 800 | 100 | 12 | 2.5 |
| 1B | 800 | 200 | 12 | 2.5 |
| 1B | 800 | 400 | 12 | 2.5 |
| 1C | 800 | 100 | 12 | 2.5 |
| 1C | 800 | 200 | 12 | 2.5 |
| 1C | 800 | 400 | 12 | 2.5 |
| 2B | 800 | 200 | 9 | 0 |
| 2C | 800 | 200 | 9 | 0 |

## 3 TEMPERATURE MEASUREMENTS

Temperatures were measured during FSW by utilising 0.5 mm diameter K type thermocouples embedded in a series of small holes (0.75 mm diameter) at a distance of 12.5 mm either side of the weld join line and for various depths (1, 2 and 3 mm) below the surface of the workpieces. All thermocouples were inserted and secured to the bottom of each hole by tape. Thermal conducting paste was packed into all holes to seat the thermocouples. Weld temperatures were then recorded digitally using a National Instruments SCXI-1000 amplifier and Labview program. Temperatures were sampled at 20 Hz. Digital smoothing was not found to be necessary to remove noise.

## 4 MECHANICAL TESTING

Mechanical characterisation of the welds was performed using two tests:

– Microhardness measurements (HV0.2) carried out mid thickness of the workpieces transverse to the weld travel direction at interval spacing of 0.5 mm.

– Uniaxial flat tensile testing.

Uniaxial flat tensile tests were performed on both the base and friction stir welded material using a Schenk-Trebel Testing Machine powered by a Zwick controller equipped with an actuator of 200 kN load capacity.

## 5 MICRO-TOMOGRAPHIC INVESTIGATION

The tomographic investigation was conducted by the GKSS-Forschungszentrum at the HASYLAB beamline W2 facility, Hamburg, Germany using a Synchrotron radiation source. Micro-computer tomographic (μCT) techniques were applied to analyse the results of the investigation.

A titanium powder measuring 30-90 microns in diameter was placed in slots milled into the interface between the 2024-T351 workpieces at both sides of the weld join line for both the top and bottom half of the workpieces. The dimensions of the slots were 10 mm in the direction of welding, 2.5 mm into each workpiece i.e. transverse to the direction of welding and 1.25 mm in height. A small quantity of the powder marker was placed into each slot and a 2024-T351 alloy plug then forced into the cavity to prevent any marker from escaping. Friction stir butt welds were then produced and evaluated using standard metallographic techniques.

A second series of experiments was then performed with the same slots milled this time into the top surface of the workpieces 1.5 mm away from the join line at various depths through the thickness of the workpieces. A small quantity of the marker material was again placed into each slot and a 2024-T351 aluminium alloy plug inserted. Shoulder type 1 in conjunction with pins B and C were then used to friction stir butt weld the workpieces. These welds were performed using a stop action technique leaving the welding pin embedded in the marker material.

## 6 RESULTS AND DISCUSSION

Macrographs representative of the friction stir welds produced using shoulder 1 and pins A, B and C can be found in Figure 3.

Weld macrographs representative of the friction stir welds produced using shoulder 2 in combination with pins B and C can be found in Figure 4. These welds were produced for a weld travel speed of 200 mm/min and an axial load of 9 kN.

The weld macrographs, Figure 3 and Figure 4 are representative of the friction stir welded structure transverse to the weld travel direction and indicate that under identical processing conditions each weld tool produces a unique and clearly identifiable weld structure. For welds produced using shoulder 1 it could be seen that pin A produced a sub-surface volumetric defect i.e. tunnel defect. This defect increased in size with increasing weld travel speed. As the size of the defect increased so did the thickness of the joined workpieces. Thinning of the workpieces was only evident for tool 1A for the weld travel speed of 100 mm/min. This thinning was no longer evident at 200 mm/min and at 400 mm/min it could clearly be seen that original height of the interface between welding tool shoulder and workpiece surface had risen by almost 1 mm.

Welding pins B and C when used in conjunction with shoulder 1, unlike pin A, demonstrated no obvious volumetric defects. Pin B had the most notable changes in

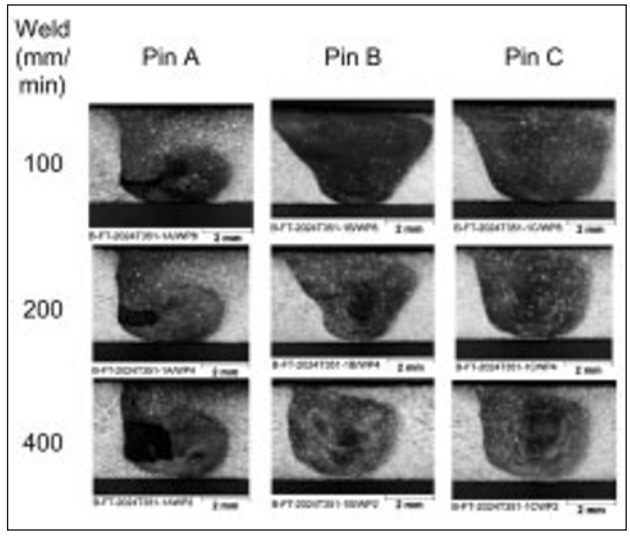


**Figure 3 – Weld macrographs produced using tool pins A, B and C in conjunction with shoulder 1 for 3 different weld travel speeds**

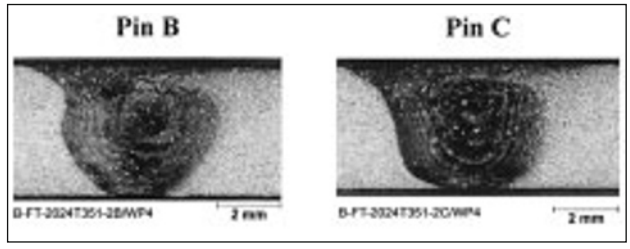


**Figure 4 – Weld macrographs produced when using tool pins B and C in conjunction with shoulder 2**

weld nugget size and shape over the three welding speeds investigated. It could also be observed that a very small lack of penetration (LOP) defect had occurred for the weld travel speed of 400 mm/min. By comparison pin C provided for the most consistent and symmetric weld nugget shape over all investigated weld travel speeds. Measurements conducted on the friction stir nugget areas indicated that for each weld travel speed pin C consistently produced the larger nugget area. This was also evident for welds produced using shoulder 2 for pins B and C, see Figure 4. These welds were produced with no evident thinning of the workpieces and were much more symmetric in shape than their counterpart welds produced using shoulder 1.

Welding temperatures measured during FSW indicated that variations in temperature could be observed for both sides of the weld join line and for the through thickness of the workpieces. The temperature measurements indicated that processing temperature varied not only in relation to weld travel speed but also as a result of welding tool configuration. A summary of peak temperatures measured 1, 2 and 3 mm below the surface of the workpieces, 12.5 mm from the weld join line and over the entire range of weld travel speeds i.e. 100-400 mm/min, are presented in Table 2.

Table 2 indicates that welds produced using tool shoulder 1 were hottest in combination with pin A but only for the advancing side of the joint line. The same series of welds were coldest for the retreating side. The friction stir welds produced using tool shoulder 1 in conjunction with pins B and C under identical welding conditions did not show such a significant variation in temperature. Here the difference in peak temperatures between the tool pins was only marginal. There were however observable differences when considering the individual values for each side of the weld. In fact all welds produced using tool 1C indicated higher welding temperatures compared to tool 1B. The higher welding temperatures produced while using tool 1C are corroborated by the fact that the weld nuggets produced using this tool were also larger in area than their counterpart nuggets produced using either tool 1A or 1B.

**Table 2 – Tool - FSW temperatures as measured 1-3 mm below workpiece surface for both sides of the joint line**

| Tool config. Shoulder / Pin | Side of joint line where measurement took place. As / Rs | Depth below surface of workpieces (mm) | Peak temp. range 100 mm/min to 400 mm/min (°C) |
|---|---|---|---|
| 1A | As | 1 | 245-210 |
| 1B | As | 1 | 230-210 |
| 1C | As | 1 | 240-210 |
| 1A | Rs | 1 | 245-180 |
| 1B | Rs | 1 | 230-195 |
| 1C | Rs | 1 | 240-205 |
| 1A | As | 2 | 245-210 |
| 1B | As | 2 | 230-210 |
| 1C | As | 2 | 240-210 |
| 1A | Rs | 2 | 245-180 |
| 1B | Rs | 2 | 230-190 |
| 1C | Rs | 2 | 240-200 |
| 1A | As | 3 | 245-180 |
| 1B | As | 3 | 230-210 |
| 1C | As | 3 | 240-195 |
| 1A | Rs | 3 | 245-160 |
| 1B | Rs | 3 | 230-190 |
| 1C | Rs | 3 | 240-200 |

Temperatures measured when FSW using tool shoulder 2 in combination with tool pins B and C indicated a much more even temperature profile between each side of the weld join line.

Microhardness (HV0.2) profiles conducted at mid thickness transverse to the weld travel direction for all welds produced using tools 1B and 1C indicated that differences in hardness were produced over the range of weld travel speeds investigated. Microhardness plots can be found in Figure 5 and Figure 6 respectively.

The microhardness profiles, in Figure 5 and Figure 6, indicate that hardness increases with increased weld travel speed. For the 2024-T351 aluminium alloy this change in hardness occurs over a travel speed range of 300 mm/min and a temperature range of approximately 50 °C. For tool 1B when welding with a weld travel speed of 400 mm/min it was found that the retreating side of the friction stir weld had the higher hardness, see Figure 5. Table 2 confirms that this is also the side having the lower peak temperatures. By comparison the same weld produced using tool 1C has the higher hard-

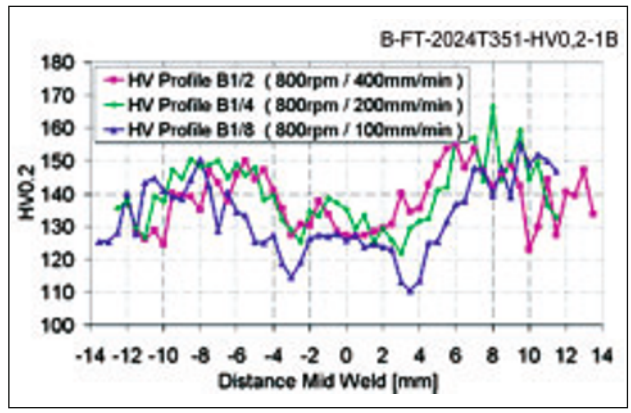


**Figure 5 – HV0.2 profiles at mid workpiece thickness for tool 1B for weld travel speeds 100, 200 and 400 mm/min**

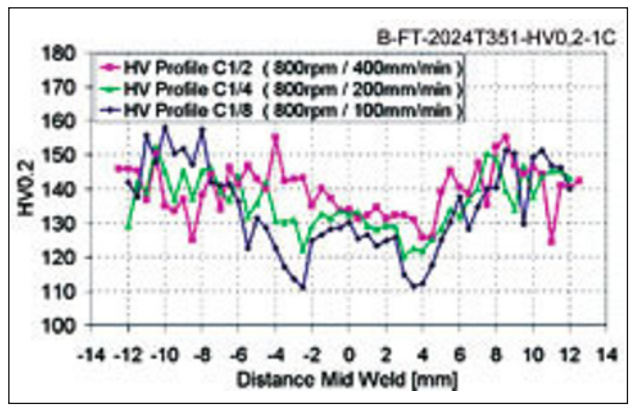


**Figure 6 – HV0.2 profiles at mid workpiece thickness for tool 1C for weld travel speeds 100, 200 and 400 mm/min**

ness values for the advancing side of the weld, see Figure 6. Table 2 similarly confirms that this is the side of the weld which exhibits the cooler processing temperatures, especially for the lower half of the workpieces i.e. measured 3 mm from the workpiece surface. The hardness of the 2024-T351 base material indicated a hardness (HV0,2) of approximately 147.

Uniaxial flat tensile tests performed on the friction stir welded specimens produced using tool 1B and 1C indicated that ultimate strength of the weld increases with increasing weld travel speed. A summary of the weld properties in relation to the base material properties can be found in Table 3. The friction stir welded specimens demonstrated yield strengths in excess of 85 % that of the base material and tensile strengths in the range between 67 % and 98 % that of the base material. If a comparison between welds produced using tools 1B and 1C for a weld travel speed of 200 mm/min is made, see Table 3, it can be seen that there exists only a small variation in the ultimate tensile strength between the two welds. If one considers yield strength however, a difference of approximately 5 % exists. In fact, for tool 1B yield strength can be seen to decrease with increasing weld travel speed. This was not the case for welds produced using tool 1C. Here the increased weld travel speed not only indicated increasing yield and ultimate tensile strength but also demonstrated an increased elongation at break of almost 70 % that of the base material. The reason as to why this had occurred is currently being investigated through a material flow visualisation study.

Macrographs were produced from friction stir welds embedded with the Ti powder marker material placed in the advancing side of the weld. These welds were undertaken to reveal if differences could be observed in marker flow patterns that could help to explain the already observed differences in temperature profiles and mechanical properties for the friction stir welds produced using tools 1B and 1C. The welds were produced for a travel speed of 200 mm/min; a welding speed which delivered high quality welds but also indicated a transition between weld properties for welds produced using tools 1B and 1C. The weld macrographs revealed some impingement of marker had occurred in relation to weld formation but only in the vicinity where the marker had originally been embedded. This could be explained due to an incomplete fit up leading to the formation of a small void between the plug and cavity containing the marker material. Although small differences had occurred between the no marker and marker embedded welds the general shape and visible characteristics associated with each weld could clearly be identified for both tool and weld parameter combinations.

**Table 3 – Tensile properties of friction stir welds produced using tool shoulder 1 in conjunction with pins B and C in comparison to the base material properties**

| Tool config. Shoulder / Pin | Weld travel speed [mm/min] | Mean Value | | |
|---|---|---|---|---|
| | | Yield Strength Rp0.2 [Mpa] | Ultimate tensile strength Rm [Mpa] | Elong. at break |
| 1B | 400 | 288 | 323 | 0.7 |
| | 200 | 295 | 442 | 8.6 |
| | 100 | 305 | 413 | 5.6 |
| 1C | 400 | 329 | 465 | 12.3 |
| | 200 | 314 | 448 | 9.0 |
| | 100 | 301 | 421 | 6.0 |
| Base material | | 333 | 478 | 18.7 |

The weld macrographs produced from the marker embedded friction stir welds revealed that tool 1C produced much less vertical displacement of the marker when compared to that produced using tool 1B. It was also evident that much larger clumps of the marker were to be found in the weld nugget produced using tool 1C. By comparison tool 1B indicated that the marker was more finely dispersed and distributed throughout both the top and bottom half of the workpieces regardless of its original location.

The weld macrographs produced with the embedded marker although capable of revealing differences in marker distribution were unable in their 2-D representation to fully describe the flow field resulting from a single friction stir weld. With this aim in mind friction stir welds were again produced having Ti powder marker material embedded for both sides of the weld joint in the top half of the workpieces. A stop action technique was now employed to halt and capture the welding pin while still in contact with the embedded marker material. A small section of the weld measuring 10 mm × 10 mm surrounding the welding tool pin was removed and examined using μCT. An example of the reconstructed Ti-powder distribution that resulted using tool 1B at a weld travel speed of 200 mm/min can be found in Figure 7.

The tomographic investigation performed on the marker embedded specimens in conjunction with the stop action technique indicated several important features pertaining to both the FSW process and the micro-tomographic analysis. The welds revealed that the marker material ahead of the welding pin was ruptured well before the pin threads made contact with it. They also revealed that the Ti powder marker flowed in the direction of tool rotation (clockwise). Marker material remained in a narrow band on the retreating side of the weld. This was not the

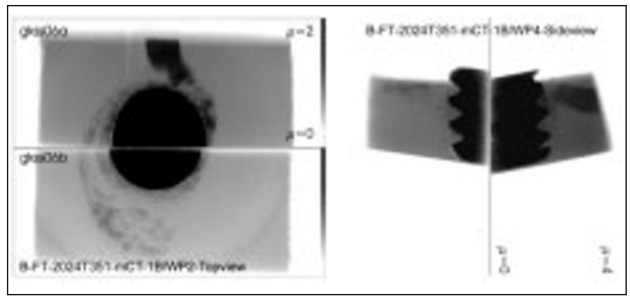

**Figure 7 – Images produced from the μCT scans; (left) top view and (right) side view of friction stir welded AA2024-T351 embedded with Ti powder marker material for top half and in the advancing side of the weld**

case for the advancing side of the weld where marker material at the workpiece surface was seen to be spread over a much wider region. A side view of the marker transport from front to back of the welding pin revealed that marker remained in intimate contact with the pin throughout the thickness of the workpiece. Marker material in front of the welding pin could be seen to be initially raised and then forced downwards from its original position in the workpieces. At the rear of the welding pin the marker appeared to be carried upwards until it came into intimate contact with the tool shoulder. It is envisaged that under the influence of the tool shoulder the marker was further distributed outwards over the surface for the advancing side of the weld. Unlike the top surface very little marker material could be seen to remain in the lower half of the workpieces behind the welding pin. Although the μCT examination of the marker embedded specimens for the stop action technique provided very useful data it was found that the energy range of the W2 beamline facility was too low to penetrate the body of the FSW pin. This meant that in order to generate 3D perspectives of marker flow multiple images needed to be produced which increased the complexity of accurately positioning the sample manipulator and this ultimately required evaluating and piecing together large numbers of images in order to capture the marker flow. For this reason it was decided to perform a second series of μCT examinations while still using the stop action welding technique. This time the major portion of the welding tool pin was removed by means of spark eroding it from the immediate weld zone. Friction stir welds were again produced for tools 1B and 1C at a weld travel speed of 200 mm/min. Images (top view) produced from this μCT investigation can be found in Figure 8.

An evaluation of the marker flow patterns, Figure 8, indicated that very significant differences existed in marker distribution not only between the FSW tools but also between marker flows for each side of a single friction stir weld. The major difference was seen to occur when FSW using tool 1B. Marker initially embedded on the advancing side of the weld was finely dispersed and deposited at the rear of the tool, again on the advancing side. Marker embedded on the retreating side however, could be seen to be distributed much more coarsely. Large clumps of the marker material could be seen to form at the rear of the welding tool again on the advancing side of the weld. Side view images produced from the μCT investigation for tool 1B and 1C also confirmed differences in the marker flow and distribution dependant on which side of the weld the marker had originated from. A comparison of the marker flow and distribution between the two tool types clearly indicated that although differences existed between the marker flows from each side of the workpieces, marker flow was much more homogeneous in nature for tool 1C. It was also observed that the deposition of the marker had been shifted closer towards the original join line interface between the workpieces while FSW using this welding tool. This differed from tool 1B where the majority of the marker material deposited at the rear of the welding pin could be seen to be biased towards the advancing side of the weld joint.

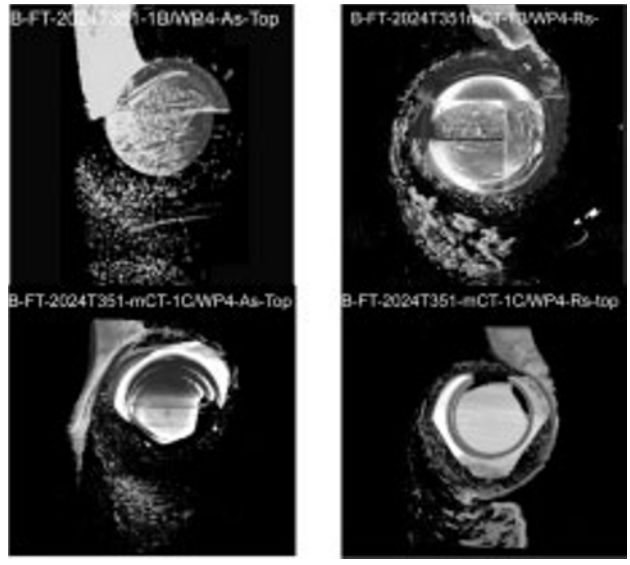


*Note Tool rotation is clockwise.*

**Figure 8 – Images (top for tool 1B and bottom for tool 1C) produced from the μCT scans performed on friction stir welds embedded with Ti powder marker where the welding tool pin was spark eroded from the weld prior to examination**

## 7 CONCLUDING REMARKS

Results of the mechanical characterisation for friction stir welds produced under identical welding parameters but having different tool pins i.e. conical threaded pin (pin B) and a conical threaded pin with three flats (pin C) indicated that a simple increase in weld travel speed alone could not account for the measured increase in ultimate tensile strength and elongation experienced by the friction stir welded 2024-T351 alloy. The fact that there existed different yielding behaviour for the welds while FSW with the different pins seemed to indicate that material flow and bonding phenomena may have been affected as a result of tool geometry. The μCT investigation has confirmed that tool geometry can have a significant effect on marker material flow and distribution throughout the friction stir weld zone.

## REFERENCES

[1] Thomas W.M., Nicholas E.D., Needham J.C., Church M.G., Templesmith P., Dawes C.J.: International Patent Application No. PCT/GB92/02203 and GB Patent Application No. 9125978.9, 1991.

[2] Guerra M., McClure J.C., Murr L.E., Nunes A.C.: Metal flow during friction stir welding. Friction stir welding and processing. Proceedings of Symposium, TMS Indianapolis, Indiana, USA, November 4-8, 2001, pp. 25-33.

[3] Krishnan K.N.: On the formation of onion rings in friction stir welds, Materials Science and Engineering, 2000, A327, pp. 246-251.

[4] Steenbergen J.E., Thornton H.R.: Quantitative determination of the conditions for hot cracking during welding of aluminium alloys, 1970, Welding Journal 49 (2), pp. 61s to 68s.